

---

# 3D Denoisers are Good 2D Teachers: Molecular Pretraining via Denoising and Cross-Modal Distillation

---

Sungjun Cho<sup>1</sup> Dae-Woong Jeong<sup>1</sup> Sung Moon Ko<sup>1</sup> Jinwoo Kim<sup>2</sup>  
Sehui Han<sup>1</sup> Seunghoon Hong<sup>2</sup> Honglak Lee<sup>1</sup> Moontae Lee<sup>1,3</sup>  
<sup>1</sup>LG AI Research <sup>2</sup>KAIST <sup>3</sup>University of Illinois Chicago

## Abstract

Pretraining molecular representations from large unlabeled data is essential for molecular property prediction due to the high cost of obtaining ground-truth labels. While there exist various 2D graph-based molecular pretraining approaches, these methods struggle to show statistically significant gains in predictive performance. Recent work have thus instead proposed 3D conformer-based pretraining under the task of denoising, which led to promising results. During downstream finetuning, however, models trained with 3D conformers require accurate atom-coordinates of previously unseen molecules, which are computationally expensive to acquire at scale. In light of this limitation, we propose D&D, a self-supervised molecular representation learning framework that pretrains a 2D graph encoder by distilling representations from a 3D denoiser. With denoising followed by cross-modal knowledge distillation, our approach enjoys use of knowledge obtained from denoising as well as painless application to downstream tasks with no access to accurate conformers. Experiments on real-world molecular property prediction datasets show that the graph encoder trained via D&D can infer 3D information based on the 2D graph and shows superior performance and label-efficiency against other baselines.

## 1 Introduction

Molecular property prediction has gained much interest across the machine learning community, leading to breakthroughs in various applications such as drug discovery [19, 29] and material design [52, 42, 50, 43]. As molecules can be represented as a *2D graph* with nodes and edges representing atoms and covalent bonds, many graph neural networks have been developed with promising results [13, 11, 7, 9, 49, 27]. However, achieving high precision requires accurate ground-truth property labels which are very expensive to obtain. This limitation has motivated adaptation of self-supervised pretraining widely used in natural language processing [12, 6] and computer vision [22, 2] onto molecular graphs with proxy objectives developed to instill useful knowledge into neural networks with unlabeled data. But existing 2D graph-based pretraining frameworks face a fundamental challenge: while the model is trained to learn representations that are invariant under various data augmentations, augmenting 2D graphs can catastrophically disrupt its topology, which renders the model unable to fully recover labels from augmented samples [57]. As a result of this limitation, recent work has shown that existing 2D pretraining approaches do not show statistically meaningful performance improvements in downstream tasks [54].

As an alternative, recent work have proposed incorporating 3D information to the pretraining objective, leveraging large unlabeled datasets of *3D conformers*, or point clouds of atoms floating in the physical space. While a natural task would be to reconstruct the input conformer, this may not induce generalizable knowledge as each conformer only represents a single local minima in a distribution of 3D configurations. On the other hand, the force field that controls the overall stabilization process provides significant chemical information that can be used across many different molecular

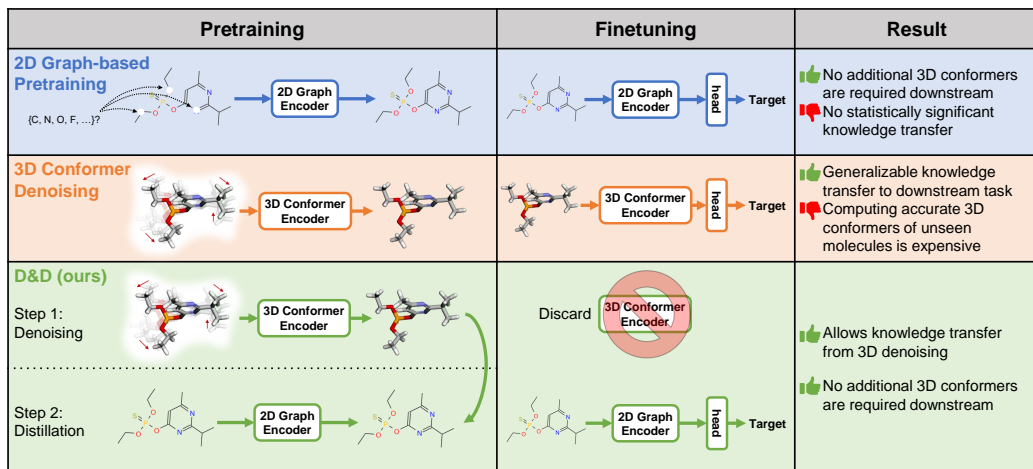


Figure 1: Comparison between D&D and existing molecular pretraining frameworks. **Top:** 2D graph-based pretraining methods fail to bring significant benefit to downstream molecular property prediction. **Middle:** 3D denoising is effective in predicting molecular properties by approximately learning the force field in the physical space, but cannot be easily applied to downstream tasks where only 2D graphs are available. **Bottom:** Our method D&D allows practitioners to leverage knowledge from 3D denoising in downstream scenarios where only 2D molecular graphs are available without the need to generate 3D conformer via expensive computations or machine learning approaches.

properties [39]. This naturally translates to pretraining via denoising conformers under perturbations, an approach that has shown state-of-the-art performance in diverse molecular property prediction benchmarks [62, 36].

Despite great performance, a model trained with denoising requires conformers downstream as well, and obtaining accurate conformers require expensive quantum mechanical computations. While there exist many rule-based [45, 33] as well as deep learning-based approaches [15, 59, 28] for generating conformers, previous work have shown that existing methods fail to generate conformers quickly and accurately enough to be used in a large scale [51].

In light of such limitations, we propose D&D (Denoise and Distill), a self-supervised molecular representation learning framework that enjoys the best of both worlds. Figure 1 shows the overall pipeline of our work. D&D sequentially performs two steps: 1) we pretrain a 3D teacher model that denoises conformers artificially perturbed with Gaussian noise and 2) freeze the 3D teacher encoder and distill representations from the 3D teacher onto the 2D student. When given a downstream task with access to 2D molecular graphs only, the 3D teacher is discarded and the 2D student is finetuned towards the given task. As a result of distillation, D&D encourages the 2D graph encoder to exploit the topology of the molecular graph towards encoding the input molecule similarly to the 3D conformer encoder without any explicit supervision from property labels. Surprisingly, experiments on various molecular property prediction datasets indicate that the 2D graph representations from D&D can generalize to unseen molecules. To the best of our knowledge, our method is the first self-supervised molecular representation learning framework that adopts cross-modal knowledge distillation to transfer knowledge from a 3D denoiser onto a 2D graph encoder. We summarize our main contributions as follows:

- We propose D&D, a two-step self-supervised molecular representation pretraining framework that performs 3D-to-2D cross-modal distillation.
- Pretraining results show that under D&D, the 2D student model can closely mimic representations from the 3D teacher model using graph features and topology. Further analysis shows that the intermediate representations of the 2D student also aligns well with 3D geometry.
- Experiments on the OGB benchmark and manually curated physical property datasets show that D&D leads to significant knowledge transfer, and also performs well in downstream scenarios where the number of labeled training data points is limited.

## 2 Related Work

In this section, we first discuss previous work on knowledge distillation that inspired our approach. We also cover existing self-supervised pretraining approaches for molecular representation learning.

**Knowledge Distillation.** Knowledge distillation (KD) was developed under the motivation of transferring knowledge learned by a large *teacher* model to a much more compact *student* model, thereby reducing the computational burden while preserving the predictive performance [23]. Example approaches in computer vision include distilling class probabilities as a soft target for classification models [1] or transferring intermediate representations of input images [56]. For dense prediction tasks such as semantic segmentation, it has been shown that a *structured* KD approach that distills pixel-level features instead leads to improvements in performance [38]. Another extension that is more closely related to our approach is *cross-modal* KD on unlabeled modality-paired data (e.g. RGB and Depth images), which was proposed to cope with modalities with limited data [18]. Inspired by this work, D&D performs 3D-to-2D cross-modal KD to allow downstream finetuning on 2D molecular graphs while utilizing the feature space refined by 3D conformer denoising. Further information on KD can be found in a recent survey by [17].

**Pretraining for Molecular Property Prediction.** Inspired by previous work in the NLP domain, there exist many self-supervised pretraining approaches for learning representations of molecular graphs. Similar to masked token prediction in BERT [12], [25] proposed node-attribute masking and context prediction to reconstruct topological structures or predict attributes of masked nodes. GROVER [46] proposed predicting what motifs exist in the molecular graph, under the insight that functional groups determine molecular properties. Contrastive approaches were also proposed, in which the task is to align representations from two augmentations of the same molecule and repel representations of different ones [21, 61]. Despite promising results, it has been shown that obtaining significant gains in performance with existing 2D pretraining methods is non-trivial, as empirical improvements rely heavily on the choice of hyperparameters and other experimental setups [54].

As molecules lie in the 3D physical space, some work have deviated from the 2D graph setting and instead proposed 3D pretraining via denoising conformers perturbed with Gaussian noise, from which empirical results have shown significant knowledge transfer to diverse molecular property prediction tasks [62, 36]. Despite great downstream performance, such 3D approaches necessitate access to accurate 3D conformers of molecules under concern, which are difficult to obtain as it requires expensive quantum mechanical computations such as density functional theory (DFT) [41].

There exist solutions to avoid these drawbacks. 3DInfomax [51] proposed cross-modal contrastive pretraining frameworks that align 2D and 3D representations. In addition to contrastive pretraining, GraphMVP [35] also incorporates generative pretraining which trains the model to reconstruct the 2D graph representation from its 3D counterpart, and vice versa. While these methods use 3D conformers during pretraining only, they do not capture information from molecular force fields, which we conjecture to be helpful for forward knowledge transfer. Our D&D framework, on the other hand, enjoys the same advantages while also leveraging generalizable knowledge obtained through conformer denoising.

## 3 Preliminaries

We first introduce preliminary information on learning representations of 2D molecular graphs and 3D molecular conformers alongside notations that we use in later sections.

**2D Molecular Graphs.** Let  $\mathcal{G} = (\mathcal{V}, \mathcal{E})$  denote the 2D molecular graph with  $N$  atoms represented as nodes in  $\mathcal{V}$ , and  $M$  bonds represented as edges in  $\mathcal{E}$ . In addition to the graph-connectivity, each node is assigned features based on chemical attributes such as atomic number and aromaticity, and similarly for each edge with features based on bond type and stereo configurations. Given the graph  $\mathcal{G}$ , a 2D graph encoder  $f^{2D}$  typically first returns representations for each node:

$$f^{2D}(\mathcal{G}) = \mathbf{Z}^{2D} \text{ where } \mathbf{Z}^{2D} \in \mathbb{R}^{N \times d}. \quad (1)$$

In molecular property prediction settings we need a single representation for each molecular graph. Typical operators used to extract graph-level representations include mean-pooling all node representations or adding a virtual node to the input graph and treating its representation as the graph representation [20].

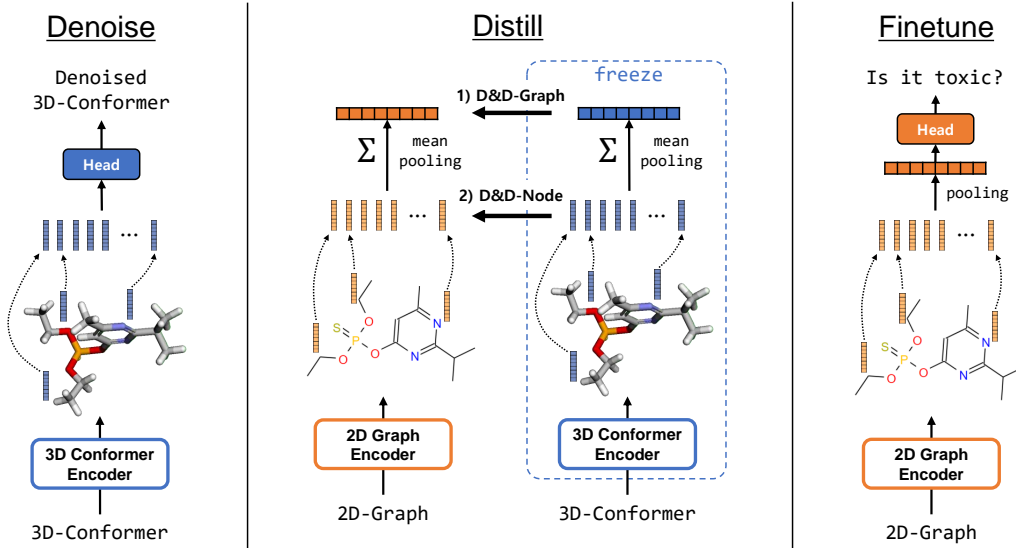


Figure 2: Illustration of our D&D framework. First we pretrain a 3D conformer encoding module by denoising perturbed conformers. Next we pretrain a 2D graph encoder by distilling representations from the 3D teacher. We propose two variants: D&D-GRAPH distills mean-pooled graph representations while D&D-NODE distills node representations in a more fine-grained manner. During finetuning, we tune the 2D graph encoder only with the given downstream data.

**3D Molecular Conformers.** Each molecule can also be represented as a 3D conformer  $\mathcal{C} = (\mathcal{V}, \mathbf{R})$  with 3D spatial coordinates of each atom stored in  $\mathbf{R} \in \mathbb{R}^{N \times 3}$ . Note that unlike in 2D graphs, 3D conformers have information on the graph connectivity nor covalent bonds in  $\mathcal{E}$ , and is instead treated as point cloud data. As with 2D graphs, let  $f^{3D}$  denote the 3D conformer encoder that takes the conformer  $\mathcal{C}$  and returns representations of each atom:

$$f^{3D}(\mathcal{C}) = \mathbf{Z}^{3D} \text{ where } \mathbf{Z}^{3D} \in \mathbb{R}^{N \times d}. \quad (2)$$

Note that how the molecule is oriented in the 3D space naturally does not affect its chemical property. Thus, the encoder  $f_{3D}$  must return representations that are invariant under rotations and translations on  $\mathbf{R}$  (i.e.  $f^{3D}(\mathcal{V}, \mathbf{R}) = f^{3D}(\mathcal{V}, g(\mathbf{R}))$  for  $g \in SE(3)$ ) for efficient weight-tying across  $SE(3)$  roto-translations. Since molecular properties are not invariant to chiral orientations, we only respect rotations and translations, but not reflections. There exist many architectures that respect  $SE(3)$  symmetry as an inductive bias [14, 5, 16, 48, 55], and any such architecture can be used for  $f^{3D}$ .

## 4 D&D: Denoise and Distill

Here we describe D&D, a molecular pretraining framework that transfers generalizable knowledge from 3D conformer denoising to a 2D graph encoder via cross-modal distillation, thereby allowing painless downstream applications without computing accurate conformers of unseen graphs. The two major steps are as follows: 1) Denoising perturbed conformers with a 3D conformer encoder  $f^{3D}$ , and 2) Distilling representations from the 3D teacher to the 2D graph encoder  $f^{2D}$ . An illustration of the overall pipeline can be found in Figure 2. As our first step of D&D is based upon previous work on conformer denoising [62, 37], we provide a brief outline of the task and refer readers to corresponding papers for further details and theoretical implications.

**Step 1: Pretraining via denoising.** Given a stabilized ground-truth conformer  $\mathcal{C} = (\mathcal{V}, \mathbf{R})$ ,  $f^{3D}$  is given as input a perturbed version of the same conformer  $\tilde{\mathcal{C}} = (\mathcal{V}, \tilde{\mathbf{R}})$ , produced by slightly perturbing the coordinates of each atom with Gaussian noise as

$$\tilde{\mathbf{R}}_i = \mathbf{R}_i + \sigma \epsilon_i \text{ where } \epsilon_i \sim \mathcal{N}(0, \mathbf{I}_3) \quad (3)$$

with noise scale  $\sigma$  as hyperparameter. Then, we attach a prediction head  $h^{3D} : \mathbb{R}^{N \times d} \rightarrow \mathbb{R}^{N \times 3}$  to the  $f^{3D}$  such that the combined model outputs 3-dimensional vectors per atom.

$$h^{3D}(f^{3D}(\tilde{\mathcal{C}})) = (\hat{\epsilon}_1, \dots, \hat{\epsilon}_N) \quad (4)$$

Lastly, the model is trained to predict the noise that has been injected to create  $\tilde{\mathcal{C}}$  from  $\mathcal{C}$ . The denoising loss minimized during training is as follows:

$$\mathcal{L}_{\text{denoise}} = \mathbb{E}_{p(\tilde{\mathcal{C}}, \mathcal{C})} \left[ \left\| h^{3\text{D}}(f^{3\text{D}}(\tilde{\mathcal{C}})) - (\epsilon_1, \dots, \epsilon_N) \right\|_2^2 \right] \quad (5)$$

where  $p(\tilde{\mathcal{C}}, \mathcal{C})$  denotes the probability distribution induced by the dataset distribution and the noise sampling procedure to create  $\tilde{\mathcal{C}}$ . Surprisingly, the denoising objective is equivalent to learning an approximation of the actual force field in the physical space derived by replacing the true distribution of conformers with a mixture of Gaussians [62]. The Gaussian mixture potential corresponds to the classical harmonic oscillator potential in physics, which is a great approximation scheme for linearized equations such as denoising.

For our experiments, we use the TorchMD-NET [55] architecture for  $f^{3\text{D}}$  following Zaidi et al. 62 due to its equivariance to SE(3) roto-translations and high performance on quantum mechanical property prediction. Note that D&D is architecture-agnostic, and any other SE(3)-equivariant architecture can be used as well.

**Step 2: Cross-modal distillation.** After pretraining via denoising is done, we distill representations from the pretrained  $f^{3\text{D}}$  to a 2D graph encoder model  $f^{2\text{D}}$ . We consider two different variants of cross-modal KD, leading to two respective variants of our approach. For the first variant D&D-GRAPH, we minimize the difference between graph representations from 2D and 3D encoders:

$$\mathcal{L}_{\text{distill-graph}} = \left\| \text{pool}(f^{2\text{D}}(\mathcal{G})) - \text{pool}(f^{3\text{D}}(\mathcal{C})) \right\|_2^2 \quad (6)$$

During training, we freeze the teacher model  $f^{3\text{D}}$  and flow gradients only through the student model  $f^{2\text{D}}$ . This effectively trains the 2D encoder to leverage the bond features and graph topology to imitate representations from 3D conformers. To obtain graph representations, we average all node representations inferred by each encoder.

Inspired by structured KD [38], we propose another variant D&D-NODE that distillation node-level representations without any pooling:

$$\mathcal{L}_{\text{distill-node}} = \left\| f^{2\text{D}}(\mathcal{G}) - f^{3\text{D}}(\mathcal{C}) \right\|_2^2 \quad (7)$$

Unlike D&D-GRAPH, D&D-NODE makes full use of the one-to-one correspondence between atoms in the molecular graph and atoms in the conformer. Hence  $f^{2\text{D}}$  is trained to align towards representations from  $f^{3\text{D}}$  in a more fine-grained manner.

For the  $f^{2\text{D}}$ , we use the TokenGT architecture that theoretically enjoys maximal expressiveness across all possible permutation-equivariant operators on 2D graphs [31]. Due to this flexibility, we expect  $f^{2\text{D}}$  to be trained to align representations from  $f^{3\text{D}}$  as closely as possible, by which we hope to see the effect of distillation to the fullest extent. Furthermore, using an attention-based architecture also allows analysis on the relationship between the attention scores of atom-pairs and their physical distance in the 3D space. Results from which are discussed later in Section 5. Note that similarly with  $f^{3\text{D}}$ , however, any other permutation-equivariant graph neural network architecture can be adopted seamlessly.

**Downstream finetuning.** Assuming the downstream task does not provide accurate conformers as input, we discard  $f^{3\text{D}}$  after the distillation step and finetune  $f^{2\text{D}}$  with molecular graphs only. We use L1 loss and BCE loss for regression and binary-classification tasks, respectively, following previous work [51].

Note that we finetune the entire  $f^{2\text{D}}$  model instead of just the newly attached prediction head on the downstream data. Given that the force fields induced by electron clouds provide knowledge that is generalizable to various molecular properties, we conjecture that D&D provides a good initial point in the parameter space from which finetuning  $f^{2\text{D}}$  entirely leads to a better local optima. This also aligns with previous observations in NLP that pretrained language models outperform models trained from scratch only when the entire model is finetuned [47].

## 5 Experiments

For empirical evaluation, we test our D&D pipeline on various molecular property prediction tasks using open-source benchmarks as well as four manually curated datasets. We also stress-test D&D under a downstream scenario where the number of labeled data points is extremely limited. All experiments are run in a remote GCP server equipped with 16 NVIDIA A100 Tensor Core GPUs.

### 5.1 Experimental Setup

**Datasets.** For pretraining, we use PCQM4Mv2 [40], a large molecule dataset consisted of 3.7M molecules. Each molecule is paired with a single 3D conformer at the lowest-energy state computed via DFT. In case of D&D, we use the same PCQM4Mv2 dataset for both denoising and distillation steps. Note that even though PCQM4Mv2 provides the HOMO-LUMO energy gap of each molecule as labels, we do not use any supervision from such labels during training, and instead treat the dataset as a collection of unlabeled molecular graph-conformer pairs.

For finetuning, we use ten benchmark datasets published in OGB [26], three of which are regression tasks and the rest are binary classification tasks. We use the same scaffold split provided by the OGB library. As shown in Appendix A, the OGB datasets exhibit different molecule distributions from PCQM4Mv2: some tasks involve atom types that the encoder has never observed during pre-training. We also manually curate four datasets on physical molecular properties: Melting point (MP) is a phase transition temperature from solid to liquid [4]. Boiling point (BP) is also a phase transition temperature from liquid to gas [32]. Refractive index (RI) measures the relative speed of light in medium to a vacuum [60]. LogP is the partition coefficient which indicates the ratio of concentrations of a compound in a mixture of two immiscible solvents, water and octanol, at equilibrium [32]. These four datasets are normalized by mean and standard deviation before training and evaluation. We randomly split the dataset 8:1:1 for training, validation and testing, respectively. The detailed dataset statistics can be found in Appendix A.

**Baselines.** We compare D&D-GRAPH and D&D-NODE against two baselines. RANDINIT is a naïve baseline that trains  $f^{2D}$  on each downstream task starting from randomly initialized model weights. 3DInfomax [51] is a contrastive pretraining approach that considers two representations, one from  $f^{2D}$  and another from  $f^{3D}$ , to be a positive pair if they result from the same molecule, or negative pair otherwise. Given a batch of molecules, it minimizes the NTXent loss introduced in SimCLR [8] to align the positive pairs together and repel the negative pairs within the feature space. For 3DInfomax, we use cosine similarity for the similarity function  $sim(\cdot, \cdot)$  and temperature  $\tau = 0.01$  for weighting negative pairs as suggested in the original paper [51].

When finetuning, we consider two pooling operators for extracting graph representations: 1) mean-pooling all node representations (+MP) and 2) using the virtual-node representation as the graph representation (+VN). For consistency, we follow the same featurization step provided by the OGB library across all experiments, which produces a 9 and 3-dimensional feature vector for each atom and bond, respectively. For reproducibility, we provide the list of hyperparameters in Appendix B.

### 5.2 Pretraining Results

Prior to downstream evaluation, we discuss interesting findings from pretraining with D&D.

**The 2D graph encoder can closely mimic representations from 3D conformers using only the molecular graph.** Figure 3 shows the training and validation loss curves of the distillation step of D&D. When pretraining with D&D-NODE, the distillation loss converges to slightly over  $10^{-2}$  with a very small generalization gap between validation and training. This shows that the 2D molecular graph contains enough information to closely imitate representations from the 3D teacher  $f^{3D}$ . The

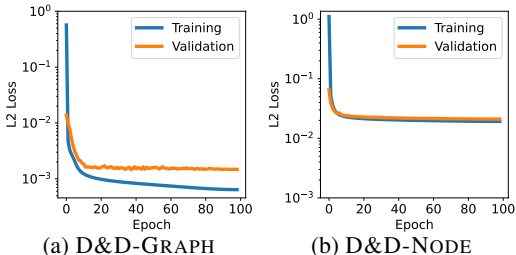


Figure 3: Training and validation loss curves during distillation of D&D-GRAPH and D&D-NODE on PCQM4Mv2. All plots are in log-scale. The 2D student is able to closely distill representations from the 3D teacher with small generalization gap.

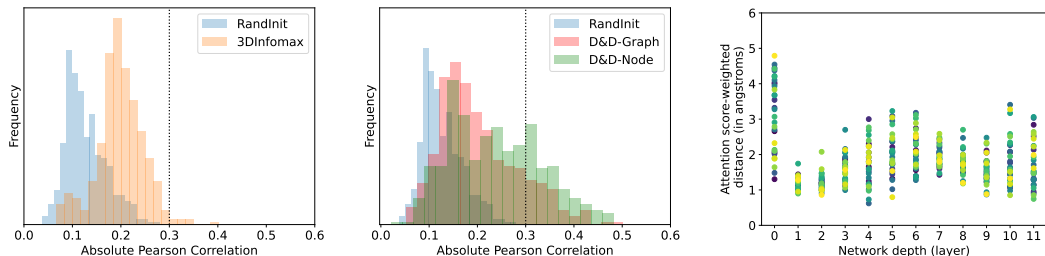


Figure 4: Histograms of Pearson correlation values between pre-softmax attention scores vs. 3D pairwise distance during inference on the PCQM4Mv2 validation set for (Left) CONTRASTIVE, (Middle) D&D-GRAPH and D&D-NODE. (Right) Average attention score-weighted 3D distances according to network depth from D&D-NODE. Each colored dot represents an attention head in the corresponding layer.

small gap between training and validation also reflects that the guidance provided via D&D-NODE can well-generalize towards unseen molecules. When pretraining with D&D-GRAPH, we find that the training loss converges to a much lower optima of  $10^{-3}$ , but with a much larger generalization gap of approximately  $10^{-3}$ . This implies that while the task of distilling mean-pooled representations is easier than distilling node-wise representations, it leads to less generalizable knowledge due to not considering the graph topological structure.

**The intermediate encoding procedure of the 2D encoder trained via D&D aligns with 3D geometry.** As we use an attention-based architecture for  $f^{2D}$ , we qualitatively assess whether the encoder processes molecular graphs as if 3D geometry without ground-truth conformers by evaluating how it performs attention across atoms during inference (e.g. do atoms nearby in the 3D space tend to attend to each other?). Specifically, we compute the absolute Pearson correlation between the 3D pairwise distances of atoms and the inner product of their features prior to the softmax layer in each attention head, averaged across all molecules in the PCQM4Mv2 validation set. Note that a larger inner product implies a relatively larger exchange of information between the two atoms. The first two figures in Figure 4 show histograms depicting distributions of averaged absolute Pearson correlation values from all attention heads for each layer in the 2D encoder after pretraining by each method. We find that 3DInfomax only leads to a slight increase in correlation compared to RANDINIT: most correlation values are distributed under 0.3. When pretrained with our D&D-variants, however, many attention heads show correlations that exceed 0.3, a value that is never reached with randomly initialized weights. This implies that our approach provides guidance to the 2D graph encoder towards processing molecular graphs while respecting its 3D geometry.

For further investigation, we also measure the average pairwise distances weighted by the attention scores from D&D-NODE with results shown in the rightmost plot in Figure 4. A higher value indicates that the attention head tends to exchange information across atoms that are far apart. Interestingly, the first layer exhibits a diverse range of distances, but the layer that immediately follows uses attention mostly to exchange information across atoms that are geometrically nearby each other, similar to a SE(3)-convolutional layer. Considering that a carbon-carbon single bond has an average length of 1.5 angstroms, this result indicates that  $f^{2D}$  pretrained with D&D-NODE can reason about 3D geometry to exchange information across atoms that are nearby in the 3D conformer, even though they may be far apart in the 2D graph.

### 5.3 Finetuning Results

Here we first provide empirical observations from downstream evaluation on OGB and Curated datasets. We also experiment on the QM9 dataset using a different 2D GNN model, to show that our pretraining approach is effective with other architectures as well.

**D&D transfers knowledge that is generalizable across diverse tasks.** Table 1 shows finetuning results on OGB, in which each experiment is averaged across 3 runs with random seeds. Comparing best results from D&D and RANDINIT, our method shows superior performance in 11 out of 12 tasks, with an average performance increase of 8.8% and 36.9% across OGB and Curated datasets, respectively. Surprisingly, when categorizing all tasks into 3 groups (OGB-regression, OGB-classification, and Curated), the tasks on which D&D shows the largest performance increase against RANDINIT from each group coincide with properties known to align well with 3D geometrical

Table 1: Average performance and standard deviations for OGB and Curated datasets: 12 tasks on the left are from OGB, and 4 tasks on the right are from manually curated data. Best results are in **bold**.

		OGB					Curated	
Dataset	Metric	ESOL RMSE(↓)	FRESOLV RMSE(↓)	LIPO RMSE(↓)	BACE ROC-AUC(↑)	BBBP ROC-AUC(↑)	BP MAE(↓)	MP MAE(↓)
RANDINIT	+MP	1.0491±0.0363	3.6445±0.0734	0.9720±0.0185	0.6360±0.1055	0.6453±0.0153	0.3000±0.0027	0.3672±0.0049
	+VN	1.1074±0.0735	3.5325±0.0453	0.9703±0.0145	0.7078±0.0284	0.6305±0.0066	0.3014±0.0052	0.3662±0.0033
3DINFOMAX	+MP	2.0037±0.1076	4.6854±0.4345	1.0167±0.0214	0.5701±0.0924	0.6238±0.0120	0.3257±0.0077	0.3862±0.0016
	+VN	1.5246±0.1092	4.2580±0.3782	0.9600±0.0206	0.6016±0.4050	0.6358±0.0088	0.3160±0.0053	0.3791±0.0022
D&D-GRAPH	+MP	<b>0.9276±0.0562</b>	<b>2.6814±0.0867</b>	0.7646±0.0126	0.6906±0.1339	0.6775±0.0117	0.2476±0.0063	0.3156±0.0017
	+VN	0.9934±0.0203	2.7004±0.0572	0.7533±0.0101	<b>0.7271±0.0721</b>	0.6714±0.0144	0.2389±0.0018	0.3096±0.0023
D&D-NODE	+MP	1.0097±0.0381	3.2935±0.2872	<b>0.6975±0.0197</b>	0.5882±0.2827	0.6754±0.0028	<b>0.2220±0.0022</b>	<b>0.2937±0.0003</b>
	+VN	1.0862±0.0887	3.4056±0.2221	0.7425±0.0113	0.6649±0.1460	<b>0.6788±0.0068</b>	0.2296±0.0068	0.2965±0.0008

Dataset	Metric	CLINTOX ROC-AUC(↑)	HIV ROC-AUC(↑)	SIDER ROC-AUC(↑)	TOX21 ROC-AUC(↑)	TOXCAST ROC-AUC(↑)	RI MAE(↓)	logP MAE(↓)
RANDINIT	+MP	0.6141±0.0290	0.7291±0.0213	0.6005±0.0058	0.7219±0.0035	0.6275±0.0046	0.1243±0.0032	0.0501±0.0043
	+VN	0.6834±0.0468	0.6758±0.0220	0.5930±0.0036	0.7190±0.0051	0.6330±0.0030	0.1250±0.0034	0.0503±0.0034
3DINFOMAX	+MP	<b>0.6919±0.0419</b>	0.7295±0.0064	0.5979±0.0086	0.6925±0.0114	0.5824±0.0069	0.1465±0.0006	0.0458±0.0010
	+VN	0.6815±0.0361	0.7165±0.0062	0.6004±0.0216	0.6979±0.0066	0.5879±0.0033	0.1344±0.0042	0.0413±0.0020
D&D-GRAPH	+MP	0.6761±0.0211	0.7766±0.0238	0.5988±0.0049	0.7541±0.0014	<b>0.6478±0.0010</b>	0.0852±0.0013	0.0274±0.0041
	+VN	0.6710±0.0429	<b>0.7771±0.0108</b>	0.6117±0.0229	0.7554±0.0003	0.6363±0.0035	0.0806±0.0048	0.0251±0.0010
D&D-NODE	+MP	0.5825±0.0257	0.7672±0.0162	0.6017±0.0113	0.7549±0.0055	0.6432±0.0038	0.0688±0.0017	<b>0.0220±0.0006</b>
	+VN	0.6594±0.0502	0.7645±0.0113	<b>0.6257±0.0106</b>	<b>0.7556±0.0068</b>	0.6421±0.0011	<b>0.0666±0.0014</b>	0.0226±0.0003

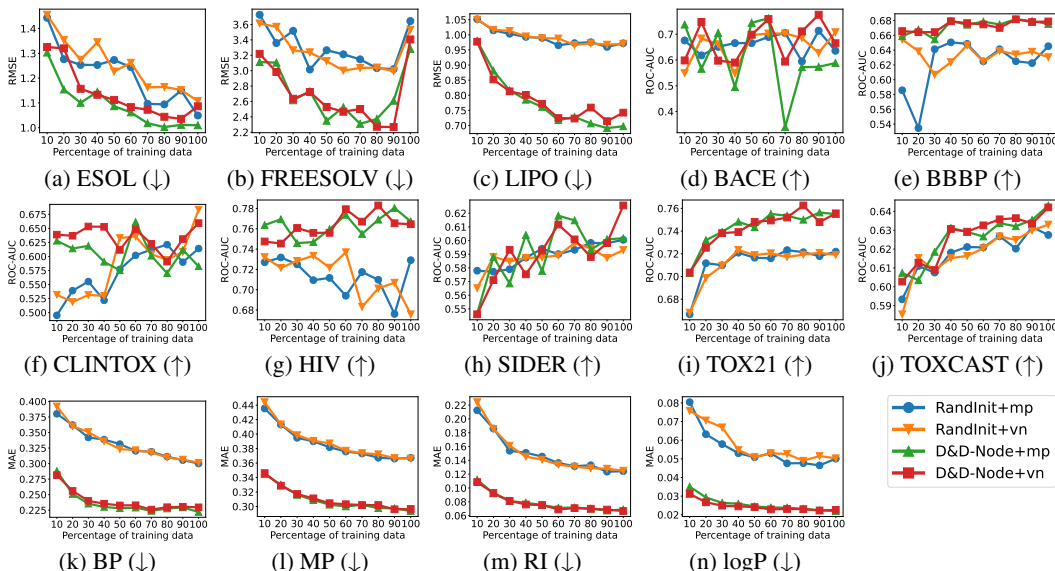


Figure 5: Experimental results demonstrating the label-efficiency of D&D on each OGB (upper two rows) and Curated (bottom-row) task. X-axes indicate the percentage of training data used for finetuning, and Y-axes show performance measurements on the respective test sets.

properties (28.1% for LIPO, 6.58% for HIV, and 55.99% for logP). For instance, solving the HIV task requires assessment of the 3D shape to estimate its binding affinity with protein pockets. Both LIPO and logP tasks are tightly associated with the overall polarity of electron clouds in the molecule, which is highly associated with the spatial positioning of the atoms. This implies that denoising followed by distillation effectively transfers 3D knowledge.

When compared against 3DInfomax, D&D shows 15.8% better performance for OGB datasets and 37.2% in Curated datasets on average. This suggests that transferring molecular-specific knowledge of force fields is much more effective than contrasting representations as a proxy task; attracting and repelling molecular representations fail to fully capture generalizable similarities and discrepancies in the chemical space. Another limitation of the contrastive approach is that the gain in performance becomes limited when only a single conformer is provided per molecule [35, 51]. This aligns well with our intuition that each conformer can be seen as a distribution of 3D configurations, and that learning a single local optima within the distribution does not provide much information. Meanwhile, D&D can learn and transfer knowledge of the overall distribution with denoising and distilling,



Table 2: Average performance and standard deviations from the QM9 quantum property prediction. Baseline results are results reported by [51]. Best results within one standard deviation are in **bold**.

Target Metric	$\mu$ MAE( $\downarrow$ )	$\alpha$ MAE( $\downarrow$ )	HOMO MAE( $\downarrow$ )	LUMO MAE( $\downarrow$ )	GAP MAE( $\downarrow$ )	R2 MAE( $\downarrow$ )	ZPVE MAE( $\downarrow$ )	$c_v$ MAE( $\downarrow$ )
RANDINIT	0.4133 $\pm$ 0.003	0.3972 $\pm$ 0.014	82.10 $\pm$ 0.33	85.72 $\pm$ 1.62	123.08 $\pm$ 3.98	22.14 $\pm$ 0.21	15.08 $\pm$ 2.83	0.1670 $\pm$ 0.004
3DINFOMAX	<b>0.3507<math>\pm</math>0.005</b>	0.3268 $\pm$ 0.006	<b>68.96<math>\pm</math>0.32</b>	<b>69.51<math>\pm</math>0.54</b>	101.71 $\pm$ 2.03	<b>17.39<math>\pm</math>0.94</b>	<b>7.966<math>\pm</math>1.87</b>	0.1306 $\pm$ 0.009
D&D-GRAPH	<b>0.3512<math>\pm</math>0.005</b>	0.2903 $\pm$ 0.029	70.36 $\pm$ 2.70	71.72 $\pm$ 2.17	98.82 $\pm$ 1.09	<b>17.61<math>\pm</math>0.68</b>	12.88 $\pm$ 3.42	<b>0.1248<math>\pm</math>0.006</b>
D&D-NODE	0.3552 $\pm$ 0.004	<b>0.2807<math>\pm</math>0.015</b>	<b>69.32<math>\pm</math>1.01</b>	<b>69.63<math>\pm</math>0.62</b>	<b>98.79<math>\pm</math>0.89</b>	<b>17.75<math>\pm</math>0.43</b>	10.19 $\pm$ 1.77	0.1429 $\pm$ 0.015

relieving practitioners from the need to obtain multiple low-energy conformers per molecule for pretraining.

**D&D enables label-efficient finetuning.** To evaluate how well D&D performs under the downstream scenario with limited number of labels, we also perform finetuning on a smaller randomly sampled subset of the original training data for each task. Figure 5 shows quantitative results of RANDINIT and D&D-NODE. In 4 out of 10 OGB tasks and all 4 Curated datasets, D&D-NODE trained with only 10% of training data shows accuracy comparable to that of RANDINIT trained on the full dataset. This demonstrates the utility of our approach in preventing overfitting to small data by leveraging generalizable knowledge from denoising. For BACE and SIDER, we find that the gain of pretraining with D&D is relatively limited compared to other tasks. While results from other OGB tasks imply that our approach can generalize towards molecules with sizes that deviate from those in PCQM4Mv2 (average 14.1 nodes per molecule for PCQM4Mv2 vs. up to 27.0 for other OGB tasks), we conjecture that too large a difference in size (vs. 34.1 for BACE and 33.6 for SIDER) between molecules may hamper generalization.

**D&D is also effective on other datasets and GNN architectures.** In addition to experiments above, we also run D&D on the QM9 benchmark [44] with 134K molecules using a different GNN architecture for the 2D student model to test whether our approach works well in a model-agnostic fashion. Specifically, we pretrain TorchMD-NET [55] on the QM9 dataset via denoising, and distill its representations from QM9 onto PNA [10], a message-passing GNN model previously used in [51]. We then finetune the pretrained 2D student to each of the properties in QM9. Note that we do not perform hyperparameter tuning for this task, but instead use the same default setting for PNA chosen by [51] including the same set of random seeds for fair comparison. More details on the experimental setup can be found in Appendix C.

In Table 2, we observe that D&D shows performs competitively against 3DInfomax on 7 out of 8 datasets. More interestingly, D&D-NODE is especially more effective than D&D-GRAPH on QM9, significantly outperforming 3DInfomax on  $\alpha$  and GAP properties. Considering that molecules in QM9 are labeled with energy-related properties through the same DFT computation used to solve their 3D atom coordinates, we conjecture that the structured-distillation approach is more well-suited to such properties by transferring atom representations in a fine-grained manner. As we propose two variants of D&D, it would be interesting to investigate whether our comparison between D&D-NODE vs. D&D-GRAPH in empirical performance aligns with domain-specific interpretations of each chemical property, which we leave as future work.

## 6 Conclusion

In this paper, we propose D&D, a novel self-supervised molecular representation learning framework that allows use of models pretrained via 3D conformer denoising towards downstream tasks that only provide 2D molecular graphs as input. As molecular force fields provide chemically generalizable information across various tasks, D&D demonstrates significant knowledge transfer to diverse molecular property prediction tasks. Additional analyses show that D&D is also highly label-efficient, showing significant performance boosts under downstream settings where the number of labeled training data is limited. As future work, we hope to extend D&D towards a multitask setting [38] to see if we can finetune a single model that performs well simultaneously across multiple molecular properties. Another exciting direction is to explore use of generative models [15, 59, 28] for molecular property prediction. Inspired by use of image diffusion models for semantic segmentation [3], it would be interesting to test whether intermediate representations inferred by diffusion-based generative models can be leveraged downstream towards generalizable knowledge transfer.

## References

- [1] Jimmy Ba and Rich Caruana. Do deep nets really need to be deep? *Advances in neural information processing systems*, 27, 2014.
- [2] Roman Bachmann, David Mizrahi, Andrei Atanov, and Amir Zamir. Multimaes: Multi-modal multi-task masked autoencoders. *arXiv preprint arXiv:2204.01678*, 2022.
- [3] Dmitry Baranchuk, Ivan Rubachev, Andrey Voynov, Valentin Khruikov, and Artem Babenko. Label-efficient semantic segmentation with diffusion models. *arXiv preprint arXiv:2112.03126*, 2021.
- [4] Jean-Claude Bradley, Antony Williams, and Andrew Lang. Jean-Claude Bradley Open Melting Point Dataset. 5 2014. doi: 10.6084/m9.figshare.1031637.v2. URL [https://figshare.com/articles/dataset/Jean\\_Claude\\_Bradley\\_Open\\_Melting\\_Point\\_Dataset/1031637](https://figshare.com/articles/dataset/Jean_Claude_Bradley_Open_Melting_Point_Dataset/1031637).
- [5] Michael M Bronstein, Joan Bruna, Taco Cohen, and Petar Veličković. Geometric deep learning: Grids, groups, graphs, geodesics, and gauges. *arXiv preprint arXiv:2104.13478*, 2021.
- [6] Tom Brown, Benjamin Mann, Nick Ryder, Melanie Subbiah, Jared D Kaplan, Prafulla Dhariwal, Arvind Neelakantan, Pranav Shyam, Girish Sastry, Amanda Askell, et al. Language models are few-shot learners. *Advances in neural information processing systems*, 33:1877–1901, 2020.
- [7] Joan Bruna, Wojciech Zaremba, Arthur Szlam, and Yann LeCun. Spectral networks and locally connected networks on graphs. 2013. doi: 10.48550/ARXIV.1312.6203. URL <https://arxiv.org/abs/1312.6203>.
- [8] Ting Chen, Simon Kornblith, Mohammad Norouzi, and Geoffrey Hinton. A simple framework for contrastive learning of visual representations. In *International conference on machine learning*, pages 1597–1607. PMLR, 2020.
- [9] Connor W. Coley, Regina Barzilay, William H. Green, Tommi S. Jaakkola, and Klavs F. Jensen. Convolutional embedding of attributed molecular graphs for physical property prediction. *Journal of Chemical Information and Modeling*, 57(8):1757–1772, 2017. doi: 10.1021/acs.jcim.6b00601. URL <https://doi.org/10.1021/acs.jcim.6b00601>. PMID: 28696688.
- [10] Gabriele Corso, Luca Cavalleri, Dominique Beaini, Pietro Liò, and Petar Veličković. Principal neighbourhood aggregation for graph nets. *Advances in Neural Information Processing Systems*, 33:13260–13271, 2020.
- [11] Michaël Defferrard, Xavier Bresson, and Pierre Vandergheynst. Convolutional neural networks on graphs with fast localized spectral filtering. 2016. doi: 10.48550/ARXIV.1606.09375. URL <https://arxiv.org/abs/1606.09375>.
- [12] Jacob Devlin, Ming-Wei Chang, Kenton Lee, and Kristina Toutanova. Bert: Pre-training of deep bidirectional transformers for language understanding. *arXiv preprint arXiv:1810.04805*, 2018.
- [13] David Duvenaud, Dougal Maclaurin, Jorge Aguilera-Iparraguirre, Rafael Gómez-Bombarelli, Timothy Hirzel, Alán Aspuru-Guzik, and Ryan P. Adams. Convolutional networks on graphs for learning molecular fingerprints. 2015. doi: 10.48550/ARXIV.1509.09292. URL <https://arxiv.org/abs/1509.09292>.
- [14] Fabian Fuchs, Daniel Worrall, Volker Fischer, and Max Welling. Se (3)-transformers: 3d roto-translation equivariant attention networks. *Advances in Neural Information Processing Systems*, 33:1970–1981, 2020.
- [15] Octavian Ganea, Lagnajit Pattanaik, Connor Coley, Regina Barzilay, Klavs Jensen, William Green, and Tommi Jaakkola. Geomol: Torsional geometric generation of molecular 3d conformer ensembles. *Advances in Neural Information Processing Systems*, 34:13757–13769, 2021.
- [16] Johannes Gasteiger, Florian Becker, and Stephan Günnemann. Gemnet: Universal directional graph neural networks for molecules. *Advances in Neural Information Processing Systems*, 34: 6790–6802, 2021.

- [17] Jianping Gou, Baosheng Yu, Stephen J Maybank, and Dacheng Tao. Knowledge distillation: A survey. *International Journal of Computer Vision*, 129(6):1789–1819, 2021.
- [18] Saurabh Gupta, Judy Hoffman, and Jitendra Malik. Cross modal distillation for supervision transfer. In *Proceedings of the IEEE conference on computer vision and pattern recognition*, pages 2827–2836, 2016.
- [19] Olgun Guvench. Computational functional group mapping for drug discovery. *Drug Discovery Today*, 21(12):1928–1931, 2016. ISSN 1359-6446. doi: <https://doi.org/10.1016/j.drudis.2016.06.030>. URL <https://www.sciencedirect.com/science/article/pii/S1359644616302483>.
- [20] W.L. Hamilton. *Graph Representation Learning*. Synthesis lectures on artificial intelligence and machine learning. Morgan & Claypool Publishers, 2020. ISBN 9781681739632. URL <https://books.google.co.kr/books?id=V6HnzQEACAAJ>.
- [21] Kaveh Hassani and Amir Hosein Khasahmadi. Contrastive multi-view representation learning on graphs. In *International Conference on Machine Learning*, pages 4116–4126. PMLR, 2020.
- [22] Kaiming He, Haoqi Fan, Yuxin Wu, Saining Xie, and Ross Girshick. Momentum contrast for unsupervised visual representation learning. In *Proceedings of the IEEE/CVF conference on computer vision and pattern recognition*, pages 9729–9738, 2020.
- [23] Geoffrey Hinton, Oriol Vinyals, Jeff Dean, et al. Distilling the knowledge in a neural network. *arXiv preprint arXiv:1503.02531*, 2(7), 2015.
- [24] Zhenyu Hou, Xiao Liu, Yukuo Cen, Yuxiao Dong, Hongxia Yang, Chunjie Wang, and Jie Tang. Graphmae: Self-supervised masked graph autoencoders. In *Proceedings of the 28th ACM SIGKDD Conference on Knowledge Discovery and Data Mining*, pages 594–604, 2022.
- [25] Weihua Hu, Bowen Liu, Joseph Gomes, Marinka Zitnik, Percy Liang, Vijay Pande, and Jure Leskovec. Strategies for pre-training graph neural networks. *arXiv preprint arXiv:1905.12265*, 2019.
- [26] Weihua Hu, Matthias Fey, Marinka Zitnik, Yuxiao Dong, Hongyu Ren, Bowen Liu, Michele Catasta, and Jure Leskovec. Open graph benchmark: Datasets for machine learning on graphs. *Advances in neural information processing systems*, 33:22118–22133, 2020.
- [27] Wengong Jin, Kevin Yang, Regina Barzilay, and Tommi Jaakkola. Learning multimodal graph-to-graph translation for molecular optimization, 2018. URL <https://arxiv.org/abs/1812.01070>.
- [28] Bowen Jing, Gabriele Corso, Jeffrey Chang, Regina Barzilay, and Tommi Jaakkola. Torsional diffusion for molecular conformer generation. *arXiv preprint arXiv:2206.01729*, 2022.
- [29] Vishnupriya Kanakaveti, Ramasamy Sakthivel, S. K. Rayala, and M. Michael Gromiha. Importance of functional groups in predicting the activity of small molecule inhibitors for bcl-2 and bcl-xl. *Chemical Biology & Drug Design*, 90(2):308–316, 2017. doi: <https://doi.org/10.1111/cbdd.12952>. URL <https://onlinelibrary.wiley.com/doi/abs/10.1111/cbdd.12952>.
- [30] Dongki Kim, Jinheon Baek, and Sung Ju Hwang. Graph self-supervised learning with accurate discrepancy learning. *arXiv preprint arXiv:2202.02989*, 2022.
- [31] Jinwoo Kim, Tien Dat Nguyen, Seonwoo Min, Sungjun Cho, Moontae Lee, Honglak Lee, and Seunghoon Hong. Pure transformers are powerful graph learners. *arXiv preprint arXiv:2207.02505*, 2022.
- [32] Sunghwan Kim, Jie Chen, Tiejun Cheng, Asta Gindulyte, Jia He, Siqian He, Qingliang Li, Benjamin A Shoemaker, Paul A Thiessen, Bo Yu, Leonid Zaslavsky, Jian Zhang, and Evan E Bolton. PubChem 2023 update. *Nucleic Acids Research*, 51(D1):D1373–D1380, 10 2022. ISSN 0305-1048. doi: 10.1093/nar/gkac956. URL <https://doi.org/10.1093/nar/gkac956>.
- [33] Greg Landrum. Rdkit: Open-source cheminformatics software. 2016. URL [https://github.com/rdkit/rdkit/releases/tag/Release\\_2016\\_09\\_4](https://github.com/rdkit/rdkit/releases/tag/Release_2016_09_4).

- [34] Han Li, Dan Zhao, and Jianyang Zeng. Kpqt: Knowledge-guided pre-training of graph transformer for molecular property prediction. *arXiv preprint arXiv:2206.03364*, 2022.
- [35] Shengchao Liu, Hanchen Wang, Weiyang Liu, Joan Lasenby, Hongyu Guo, and Jian Tang. Pre-training molecular graph representation with 3d geometry. *arXiv preprint arXiv:2110.07728*, 2021.
- [36] Shengchao Liu, Hongyu Guo, and Jian Tang. Molecular geometry pretraining with se (3)-invariant denoising distance matching. *arXiv preprint arXiv:2206.13602*, 2022.
- [37] Shengchao Liu, Meng Qu, Zuobai Zhang, Huiyu Cai, and Jian Tang. Structured multi-task learning for molecular property prediction. In *International Conference on Artificial Intelligence and Statistics*, pages 8906–8920. PMLR, 2022.
- [38] Yifan Liu, Changyong Shu, Jingdong Wang, and Chunhua Shen. Structured knowledge distillation for dense prediction. *IEEE transactions on pattern analysis and machine intelligence*, 2020.
- [39] Paul G. Mezey. Distributions and averages of molecular conformations. *Computers & Chemistry*, 25(1):69–75, 2001. ISSN 0097-8485. doi: [https://doi.org/10.1016/S0097-8485\(00\)00089-9](https://doi.org/10.1016/S0097-8485(00)00089-9). URL <https://www.sciencedirect.com/science/article/pii/S0097848500000899>.
- [40] Maho Nakata and Tomomi Shimazaki. Pubchemqc project: A large-scale first-principles electronic structure database for data-driven chemistry. *Journal of Chemical Information and Modeling*, 57(6):1300–1308, 2017. doi: 10.1021/acs.jcim.7b00083. URL <https://doi.org/10.1021/acs.jcim.7b00083>. PMID: 28481528.
- [41] Robert G Parr and Yang Weitao. *Density-Functional Theory of Atoms and Molecules*. Oxford University Press, 01 1995. ISBN 9780195092769. doi: 10.1093/oso/9780195092769.001.0001. URL <https://doi.org/10.1093/oso/9780195092769.001.0001>.
- [42] Edward O. Pyzer-Knapp, Kewei Li, and Alan Aspuru-Guzik. Learning from the harvard clean energy project: The use of neural networks to accelerate materials discovery. *Advanced Functional Materials*, 25(41):6495–6502, 2015. doi: <https://doi.org/10.1002/adfm.201501919>. URL <https://onlinelibrary.wiley.com/doi/abs/10.1002/adfm.201501919>.
- [43] Edward O. Pyzer-Knapp, Jed W. Pitera, Peter W. J. Staar, Seiji Takeda, Teodoro Laino, Daniel P. Sanders, James Sexton, John R. Smith, and Alessandro Curioni. Accelerating materials discovery using artificial intelligence, high performance computing and robotics. *npj Computational Mathematics*, 8:84, January 2022. doi: 10.1038/s41524-022-00765-z.
- [44] Raghunathan Ramakrishnan, Pavlo O Dral, Matthias Rupp, and O Anatole Von Lilienfeld. Quantum chemistry structures and properties of 134 kilo molecules. *Scientific data*, 1(1):1–7, 2014.
- [45] Sereina Riniker and Gregory A. Landrum. Better informed distance geometry: Using what we know to improve conformation generation. *Journal of Chemical Information and Modeling*, 55(12):2562–2574, 2015. doi: 10.1021/acs.jcim.5b00654. URL <https://doi.org/10.1021/acs.jcim.5b00654>. PMID: 26575315.
- [46] Yu Rong, Yatao Bian, Tingyang Xu, Weiyang Xie, Ying Wei, Wenbing Huang, and Junzhou Huang. Self-supervised graph transformer on large-scale molecular data. *Advances in Neural Information Processing Systems*, 33:12559–12571, 2020.
- [47] Danielle Rothmel, Margaret Li, Tim Rocktäschel, and Jakob Foerster. Don’t sweep your learning rate under the rug: A closer look at cross-modal transfer of pretrained transformers. *arXiv preprint arXiv:2107.12460*, 2021.
- [48] Victor Garcia Satorras, Emiel Hoogeboom, and Max Welling. E(n) equivariant graph neural networks. In *International conference on machine learning*, pages 9323–9332. PMLR, 2021.
- [49] Franco Scarselli, Marco Gori, Ah Chung Tsoi, Markus Hagenbuchner, and Gabriele Monfardini. The graph neural network model. *IEEE Transactions on Neural Networks*, 20(1):61–80, 2009. doi: 10.1109/TNN.2008.2005605.

- [50] Jonathan Schmidt, Mário R. G. Marques, Silvana Botti, and Miguel A. L. Marques. Recent advances and applications of machine learning in solid-state materials science. *npj Computational Mathematics*, 5:83, August 2019. doi: 10.1038/s41524-019-0221-0.
- [51] Hannes Stärk, Dominique Beaini, Gabriele Corso, Prudencio Tossou, Christian Dallago, Stephan Günnemann, and Pietro Liò. 3d infomax improves gnns for molecular property prediction. In *International Conference on Machine Learning*, pages 20479–20502. PMLR, 2022.
- [52] Changwon Suh, Clyde Fare, James A. Warren, and Edward O. Pyzer-Knapp. Evolving the materials genome: How machine learning is fueling the next generation of materials discovery. *Annual Review of Materials Research*, 50(1):1–25, 2020. doi: 10.1146/annurev-matsci-082019-105100. URL <https://doi.org/10.1146/annurev-matsci-082019-105100>.
- [53] Mengying Sun, Jing Xing, Huijun Wang, Bin Chen, and Jiayu Zhou. Mocl: Data-driven molecular fingerprint via knowledge-aware contrastive learning from molecular graph. In *Proceedings of the 27th ACM SIGKDD Conference on Knowledge Discovery & Data Mining*, pages 3585–3594, 2021.
- [54] Ruoxi Sun. Does gnn pretraining help molecular representation? *arXiv preprint arXiv:2207.06010*, 2022.
- [55] Philipp Thölke and Gianni De Fabritiis. Torchmd-net: Equivariant transformers for neural network based molecular potentials. *arXiv preprint arXiv:2202.02541*, 2022.
- [56] Yonglong Tian, Dilip Krishnan, and Phillip Isola. Contrastive representation distillation. *arXiv preprint arXiv:1910.10699*, 2019.
- [57] Puja Trivedi, Ekdeep Singh Lubana, Mark Heimann, Danai Koutra, and Jayaraman J Thiagarajan. Analyzing data-centric properties for contrastive learning on graphs. *arXiv preprint arXiv:2208.02810*, 2022.
- [58] Jun Xia, Lirong Wu, Jintao Chen, Bozhen Hu, and Stan Z Li. Simgrace: A simple framework for graph contrastive learning without data augmentation. In *Proceedings of the ACM Web Conference 2022*, pages 1070–1079, 2022.
- [59] Minkai Xu, Lantao Yu, Yang Song, Chence Shi, Stefano Ermon, and Jian Tang. Geodiff: A geometric diffusion model for molecular conformation generation. *arXiv preprint arXiv:2203.02923*, 2022.
- [60] Carl L. Yaws. Chapter 1 - physical properties – organic compounds. In Carl L. Yaws, editor, *The Yaws Handbook of Physical Properties for Hydrocarbons and Chemicals (Second Edition)*, pages 1–683. Gulf Professional Publishing, Boston, second edition edition, 2015. ISBN 978-0-12-800834-8. doi: <https://doi.org/10.1016/B978-0-12-800834-8.00001-3>. URL <https://www.sciencedirect.com/science/article/pii/B9780128008348000013>.
- [61] Yuning You, Tianlong Chen, Yongduo Sui, Ting Chen, Zhangyang Wang, and Yang Shen. Graph contrastive learning with augmentations. *Advances in Neural Information Processing Systems*, 33:5812–5823, 2020.
- [62] Shehryar Zaidi, Michael Schaarschmidt, James Martens, Hyunjik Kim, Yee Whye Teh, Alvaro Sanchez-Gonzalez, Peter Battaglia, Razvan Pascanu, and Jonathan Godwin. Pre-training via denoising for molecular property prediction. *arXiv preprint arXiv:2206.00133*, 2022.
- [63] Zaixi Zhang, Qi Liu, Hao Wang, Chengqiang Lu, and Chee-Kong Lee. Motif-based graph self-supervised learning for molecular property prediction. *Advances in Neural Information Processing Systems*, 34:15870–15882, 2021.
- [64] Jinhua Zhu, Yingce Xia, Lijun Wu, Shufang Xie, Tao Qin, Wengang Zhou, Houqiang Li, and Tie-Yan Liu. Unified 2d and 3d pre-training of molecular representations. In *Proceedings of the 28th ACM SIGKDD Conference on Knowledge Discovery and Data Mining*, pages 2626–2636, 2022.

## Answers to Potential Questions

To provide a better understanding of our draft, we start the supplementary material by providing answers to potential questions on the overall motivation of our work, our proposed methodology, and presented empirical results. We hope most questions during review can be answered in this section, and would be happy to clarify any further questions during the author response period as well. Further supplementary material can be found in the following sections.

### **Q1: What is novel about D&D, considering that it combines pretraining via denoising [62] and cross-modal distillation [18] from previous work?**

**A1:** While the two components D&D are indeed from separate existing work, our work is the first to combine the two techniques for molecular property prediction and show that denoising 3D conformers can be used independently as a powerful pretraining objective that transfers generalizable knowledge to 2D graph encoders for molecular property prediction. Unlike previous methods, D&D allows 2D graph encoders to learn force fields on the 3D space, the information from which we conjecture to be critical in molecular property prediction. Experiments with OGB and QM9 testbeds show that our approach is effective despite its simplicity.

### **Q2: Why is using one conformer per molecule better? Why not use more conformers for D&D?**

**A2:** Using less conformers is better in terms of efficiency since each conformer requires expensive optimizations via DFT. Therefore, we test D&D on a setting where each molecule only has one conformer. Nonetheless, D&D can still be used with multiple conformers per molecule, in which case we expect to see performance improvements as denoising from multiple local optima can give a broader information on the force field of the molecule.

### **Q3: What are the node and edge features used for molecular graphs?**

**A3:** We use the featurization pipeline provided by the OGB library [26]. For reference, below is a list of node- and edge-features used in our experiments:

- 9 node features: atomic number, chirality, degree, charge, number of hydrogens attached, number of radical electrons, hybridization, aromaticity, in a ring.
- 3 edge features: bond type, bond stereo configuration, conjugation

### **Q4: D&D should be evaluated using more baselines and architectures.**

**A4:** We are aware of many other baselines such as GraphMVP [35], GraphMAE [24], MGSSL [63], SimGRACE [58], MoCL [53], D-SLA [30], UnifiedMol [64], and KPGT [34]. For this paper, however, we chose 3DInfomax [51] as a representative baseline due to it being the first to propose a molecular representation learning pipeline that uses 3D conformers only during pretraining. While we chose to mainly test D&D using a global-attention based architecture (*i.e.* TokenGT), integrating its implementation with other pretraining techniques is a significant bottleneck at this time, but we hope to run further experiments soon. We also hope to test D&D with message-passing GNNs (*i.e.* GCN, GIN, GraphSAGE), but for this work, we focus on training with TokenGT[31] due to its strong theoretical expressiveness that allows distilling 3D conformer representations as closely as possible.

### **Q5: Why does D&D use L1- and BCE-loss for regression and classification for finetuning?**

**A5:** These choices of loss functions are from previous work [51]. While it is possible to add additional loss terms for D&D such as regularization, we follow the same choices for fair comparison. Furthermore, we do not use additional loss terms to directly examine the overall quality of pretrained representations from the 3D denoiser.

### **Q6: How much overlap is there between each curated dataset vs. PCQM4Mv2?**

**A6:** In Table 3, we provide data overlap measurements of our curated datasets against the pretraining PCQM4Mv2 dataset in 3 different aspects: *Elements* shows the percentage of elements in each dataset that also appears in PCQM4Mv2. *Composition* shows a similar percentage in molecular composition instead, which is computed by the number of each element present in the molecule (excluding hydrogen atoms). Lastly, *Molecule* measures the percentage of full molecules that are also in PCQM4Mv2 (matched via canonical SMILES). In terms of element coverage, we find that 50% of elements in BP are not observed during pretraining on PCQM4Mv2, while other datasets show larger overlap. The compositional overlaps are overall much higher, which implies that the molecular sizes are relatively similar. Lastly, each curated dataset shows an overlap of 10% to 20% in actual molecules, with logP showing the least overlap of 6.32%.

Table 3: Overlap between 4 curated datasets and PCQM4Mv2.

Dataset	BP	MP	RI	logP
Elements	50.0%	65.2%	100.0%	68.2%
Composition	95.0%	79.2%	96.1%	81.8%
Molecule	22.4%	11.5%	18.1%	6.32%

### Q7: Performances fluctuate between D&D-GRAPH and D&D-NODE. What would be the preferred approach given a new target?

A7: Unfortunately, we do not have an intuitive way to choose the better setting for distillation and thus would need to pick through hyperparameter tuning, but we conjecture that the preferred approach may be aligned with chemical characteristics of the target molecular property. This is supported by our QM9 experiments which show that D&D-NODE is overall superior to D&D-GRAPH for quantum properties, which aligns with previous observations where accurate atom-wise coordinates are needed for high-quality prediction for such targets [51]. A deeper understanding of domain-knowledge would allow us to make similar analogies for physical chemistry, physiology, or biophysics targets in OGB, but for now we leave such further analysis as future work.

## A Dataset Statistics

In Table 4, we provide basic statistics of each pretraining and finetuning dataset.

Table 4: Statistics of every dataset used in our experiments.

Dataset	# of molecules	Avg. # of Atoms	Avg. # of Bonds	# of Elements	Task (Metric)	# of Targets
PCQM4Mv2	3,378,309	14.1	14.6	19	-	-
ESOL	1,128	13.3	13.7	9	Regression (RMSE)	1
LIPO	4,200	27.0	29.5	12		1
FREESOLV	642	8.7	8.4	9		1
BACE	1,513	34.1	36.9	8	Binary Classification (ROC-AUC)	1
BBBP	2,039	24.1	26.0	13		1
CLINTOX	1,477	26.2	27.9	28		2
HIV	41,127	25.5	27.5	55		1
SIDER	1,427	33.6	35.4	40		27
TOX21	7,831	18.6	19.3	51		12
TOXCAST	8,576	18.8	19.3	53		617
BP	7,111	11.1	10.8	28		1
MP	21,744	15.7	16.4	22	1	
RI	7,304	12.6	12.5	6	Regression (MAE)	1
logP	29,458	40.5	40.5	19		1
QM9	130,831	18.0	37.3	5		8

## B Hyperparameters

Table 5 shows the hyperparameters used for our experiments.

Table 5: Hyperparameter settings used (a,b) for the 3D teacher and 2D student architectures, (c) training parameters used for all 3 steps of D&amp;D.

(a) 3D Teacher TorchMD-Net		(b) 2D Student TokenGT		(c) Training Setup	
Parameter	Value	Parameter	Value	Parameter	Value
# of layers	8	# of layers	12	# of Epochs	100
# of heads	8	# of heads	32	Batch Size	128
Embed. Dim	768	Embed. Dim.	128	Learning Rate	5e-4
# of rbf kernels	64			Layer Decay	0.65
Batch size	70			Weight Decay	0.05
# of epochs	30			Warmup Epochs	5
LR	1e-7			LR Scheduler	Cosine
LR Scheduler	Cosine			Optimizer	AdamW
Warmup steps	10000				

## C QM9 Quantum Property Prediction

For further comparison, we test D&D on the QM9 quantum property prediction task. We use the same training setup used by Stärk et al. [51]. Note that 3DInfomax previously used the PNA [10] architecture, which performs graph convolution with multiple message aggregators. As reference, we provide a list of baselines previously tested in [51] below:

- RANDINIT: Randomly initialized weights.
- GRAPHCL [61]: Contrastive loss to align representations under graph augmentations.
- PROPRED: Predicting the Gibbs free energy
- DISPRED: Predicting all atom-pairwise distances
- CONFGEN [15]: Generating 10 conformers per molecule

Note that these baselines are trained on the GEOM-Drugs pretraining subset consisted of 140k molecules unlike 3DInfomax and D&D, which are trained on a 50k subset of QM9. For D&D, we train a TorchMD-NET on the same pretraining subset as our 3D teacher, and distill its representations to PNA.

Table 6 shows the full results. We find that similar to 3DINFOMAX, DND-NODE consistently results in positive knowledge transfer, as it outperforms RANDINIT across all QM9 tasks. When comparing to 3DINFOMAX, we find significant performance boosts in 6 out of 8 tasks, and competitive accuracy in the other two. We find that the largest performance gain occurs in the ALPHA task. This shows that our approach of distilling representations from 3D conformers to 2D encoders is valid not only for attention-based graph encoding architectures, but for convolution-based GNNs as well.

Table 6: Test evaluation results on each QM9 quantum property prediction dataset. The baseline results are from Stärk et al. 51. D&D results are from using the same set of seeds used by the baselines. Best results and results within one standard deviation are in **bold**.

Target Metric	$\mu$ MAE(↓)	$\alpha$ MAE(↓)	HOMO MAE(↓)	LUMO MAE(↓)	GAP MAE(↓)	R2 MAE(↓)	ZPVE MAE(↓)	$c_v$ MAE(↓)
RANDINIT	0.4133	0.3972	82.10	85.72	123.08	22.14	15.08	0.1670
GRAPHCL	0.3937	0.3295	79.57	80.81	120.08	21.84	12.39	0.1422
PROPREP	0.3975	0.3732	93.11	99.84	131.99	29.21	11.17	0.1795
DISPRED	0.4626	0.3570	80.58	84.93	116.21	29.23	25.91	0.1587
CONFGEN	0.3940	0.4219	79.75	79.16	110.72	20.86	21.10	0.1555
3DINFOMAX	<b>0.3507±0.005</b>	0.3268±0.006	<b>68.96±0.32</b>	<b>69.51±0.54</b>	101.71±2.03	<b>17.39±0.94</b>	<b>7.966±1.87</b>	0.1306±0.009
D&D-GRAPH	<b>0.3512±0.005</b>	0.2903±0.029	70.36±2.70	71.72±2.17	98.82±1.09	<b>17.61±0.68</b>	12.88±3.42	<b>0.1248±0.006</b>
D&D-NODE	0.3552±0.004	<b>0.2807±0.015</b>	<b>69.32±1.01</b>	<b>69.63±0.62</b>	<b>98.79±0.89</b>	<b>17.75±0.43</b>	10.19±1.77	0.1429±0.015